Effect of structural defects consisting of ternary mixed crystals on localized interface optical modes in superlattices

Ke-Qiu Chen,[1,2,*] Xue-Hua Wang,[1] and Ben-Yuan Gu[3]
[1] *Institute of Physics, Chinese Academy of Sciences, P.O. Box 603, Beijing 100080, China*
[2] *Department of Physics, Tsinghua University, Beijing 100084, China*
[3] *CCAST (World Laboratory), P.O. Box 8730, Beijing 100080, China*
and Institute of Physics, Chinese Academy of Sciences, P.O. Box 603, Beijing 100080, China
(Received 5 July 2001; published 27 March 2002)

The localized interface optical-phonon modes lying in a minigap of AlAs-GaAs superlattice with structural defects consisting of ternary mixed-crystal $Al_xGa_{1-x}As$ are studied in the dielectric continuum approximation. We find that three localized interface optical modes appear in each frequency minigap for certain structural parameters. Two of them are antisymmetric with respect to the center of the defect layers and display interesting features significantly different from those in the structure with a binary crystal defect layer. However, the third mode with symmetric property shows similar behavior as that in the structure with a binary crystal defect layer.

DOI: 10.1103/PhysRevB.65.153305 PACS number(s): 63.20.Pw, 63.20.Dj, 63.22.+m

In the past two decades, the vibrational properties in superlattices (SL's) have attracted much attention due to their novel physical properties in comparison with bulk materials and potential applications. As far as optical phonons are concerned, their characteristics in various SL structures have been extensively investigated. It has become a well-known fact that the optical-phonon modes in a SL can be divided into two types: One is a type of bulklike modes, the other a type of interface optical modes.[1,2] The bulklike modes confined to different slabs are completely decoupled, while the interface optical-phonon modes (IOPM's) extend over the whole structure. The IOPM's have been found to play a dominant role in electron-phonon interactions in quantum wells and superlattices.[3–7] The dispersion relation of IOPM's has been extensively analyzed in terms of the dielectric continuum model theoretically,[8–12] and the IOPM's predicated by theoretical models have been observed by means of Raman scattering.[13–16]

Recently, one of the extremely interesting subjects is to study the properties of localized vibrational modes in a superlattice with the presence of inhomogeneities such as surface, interface, or defect layer. Some authors have investigated localized acoustic modes of different samples such as in a finite layered structure with defect layers,[17–19] in semi-infinite SL's with a substrate or an adsorbed layer,[20] and in infinite SL's with structural defects.[21] Surface phonon polaritons have been studied within two-layer[22] and three-layer SL's.[23]

Very recently, the authors[24] studied the localized IOPM's in SL's with structural defects. Here, we will extend our previous work and investigate the effects of the defect layer consisting of ternary mixed crystal $Al_xGa_{1-x}As$ on the localized IOPM's in detail. The ternary mixed-crystal system is usually used in heterostructures and SL's. Many properties of the ternary mixed crystals are different from those of binary crystals and they can be modulated by changing the mole fractions of the compounds. It is well known that the long-wavelength optical phonons in ternary mixed crystal $Al_xGa_{1-x}As$ exhibit the so-called two-mode behavior. Our investigation shows that the effects of the mixed crystal changes substantially the localized IOPM's in the SL's.

We now consider such a structural defect SL as $\cdots|b|a|b|a|\mathbf{d}|a|b|a|b|\cdots$, in which a defect layer labeled as **d** (material $Al_xGa_{1-x}As$) with a thickness of W_d is embedded between two semi-infinite SL's with the unit cell composed of a(GaAs) and b(AlAs) material. The thicknesses of constituent layers a and b are W_a and W_b, respectively, and the superlattice period is $W=W_a+W_b$.

In the following, we numerically examine the effects of the structural defect layer consisting of ternary mixed crystal $Al_xGa_{1-x}As$ on the localized IOPM's in accordance with the formulas derived in Ref. 24. In the calculations, we employ those values of dielectric constants and phonon frequencies of GaAs, AlAs, and $Al_xGa_{1-x}As$ referred to in Refs. 12 and 25: $\epsilon_\infty(\mathrm{GaAs})=10.89$ and $\epsilon_\infty(\mathrm{AlAs})=8.16$, $\omega_{LO}(\mathrm{GaAs})=55.045$ THz, $\omega_{TO}(\mathrm{GaAs})=50.5503$ THz, $\omega_{LO}(\mathrm{AlAs})=76.0608$ THz, and $\omega_{TO}(\mathrm{AlAs})=68.150$ THz; while $Al_xGa_{1-x}As$ has both AlAs-like and GaAs-like modes:

$$\omega_{LO}(\mathrm{GaAs\text{-}like})=55.045-9.9461x+2.7181x^2, \quad (1)$$

$$\omega_{TO}(\mathrm{GaAs\text{-}like})=50.5503-0.9718x-1.7614x^2, \quad (2)$$

$$\omega_{LO}(\mathrm{AlAs\text{-}like})=67.7699+13.3323x-5.0414x^2, \quad (3)$$

$$\omega_{TO}(\mathrm{AlAs\text{-}like})=67.7699+0.8352x-0.4555x^2. \quad (4)$$

Note that the frequencies cited correspond to $q=0$. The value of dielectric constant of $Al_xGa_{1-x}As$ is evaluated by

$$\epsilon_\infty(Al_xGa_{1-x}As)=10.89-2.73x. \quad (5)$$

The dielectric functions of a binary crystal and a ternary mixed crystal are expressed in the form of[26,27]

$$\epsilon_i(\omega)=\epsilon_{\infty i}\frac{(\omega^2-\omega_{LOi}^2)}{(\omega^2-\omega_{TOi}^2)} \qquad (i=a,b) \quad (6)$$

and

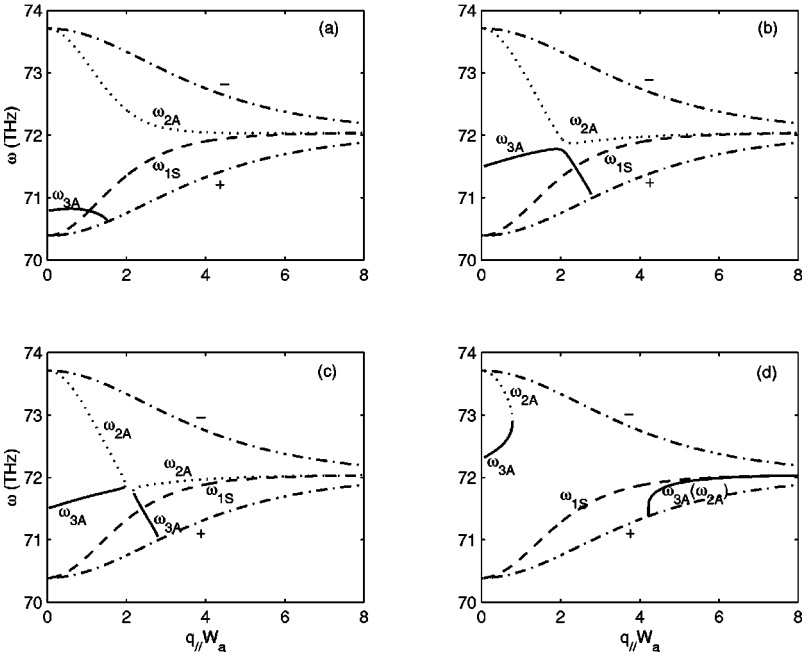

FIG. 1. Calculated frequencies of localized IOPM's lying in the AlAs-like minigap as a function of the transverse wave number $q_{//}$ for different concentrations x of defect layer. (a)–(d) correspond to $x=0.25,0.317,0.318$, and 0.40, respectively. The dashed curves (labeled ω_{1S}) represent the localized IOPM's with even parity, while the dotted and solid curves (labeled ω_{2A} and ω_{3A}, respectively) denote localized IOPM's with odd parity. The dot-dashed curves represent the band edge of the minigap. The region between the two dot-dashed curves represents the frequency minigap. The signs + and − represent the even and odd parities, respectively.

$$\epsilon(\omega)=\epsilon_{\infty}\frac{(\omega^2-\omega_{LOa}^2)(\omega^2-\omega_{LOb}^2)}{(\omega^2-\omega_{TOa}^2)(\omega^2-\omega_{TOb}^2)}, \tag{7}$$

respectively, where ωLOi(ωTOi) is the longitudinal (transverse) optical-phonon frequency of the binary crystal, and $\epsilon_{\infty i}$ the optical dielectric constant of the material $i(i=a,b)$. The two-mode behavior of ternary mixed crystal in Eq. (7) is distinguished by subscripts a and b which respectively stand for GaAs-like and AlAsS-like modes.

Figures 1 and 2 show the dependence of the localized IOPM's lying in AlAs-like and GaAs-like minigaps on the transverse wave number $q_{//}$ for different concentrations x. Here, we take $W_a=20$ nm, $W_b=8$ nm, and $W_d=3$ nm. From Fig. 1, it can be clearly seen that there are three branches of the localized IOPM's, labeled as ω_{1S}, ω_{2A}, and ω_{3A}, respectively, lying in the minigap for certain structural parameters and transverse wave numbers. Macroscopic electrostatic potential for ω_{1S} branch is symmetric and both ω_{2A} and ω_{3A} branches are antisymmetric with respect to the center of the defect layer, respectively. The number of localized IOPM's obtained here is remarkably different from that obtained in Ref. 24 where only two localized IOPM's are survival. In Ref. 24, the structural defect layer is different from constituent layers only in thickness. In this present work, however, the structural defect layer is made of ternary mixed crystal $Al_xGa_{1-x}As$, where the AlAs-like (GaAs-like) mode frequencies are different from the AlAs (GaAs) mode frequencies in regions adjacent to the defect layer, so it can be

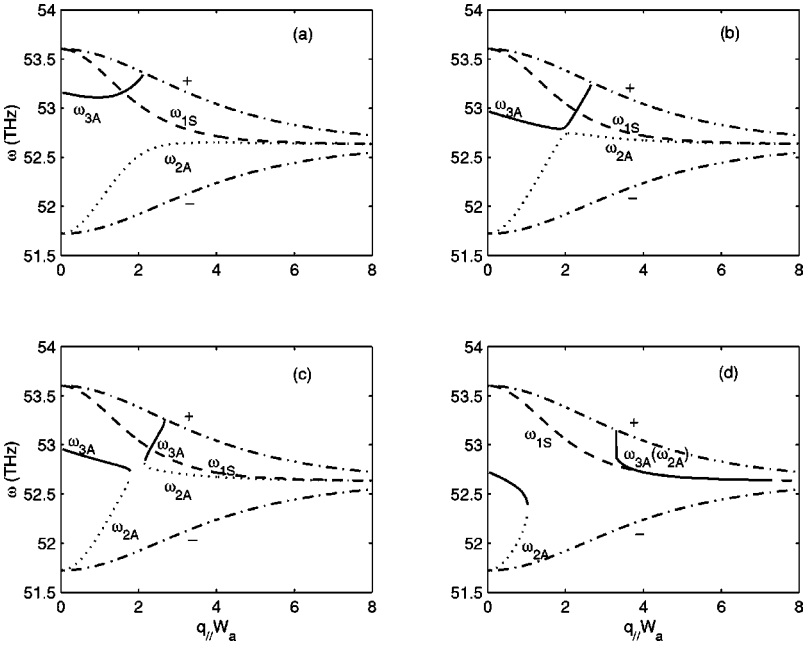

FIG. 2. Calculated frequencies of localized IOPM's lying in the GaAs-like minigap as a function of the transverse wave number $q_{//}$ for different concentrations x of the defect layer. (a)–(d) correspond to $x=0.20$, 0.222, 0.223, and 0.25, respectively. Explanations for all curves are the same as for Fig. 1.

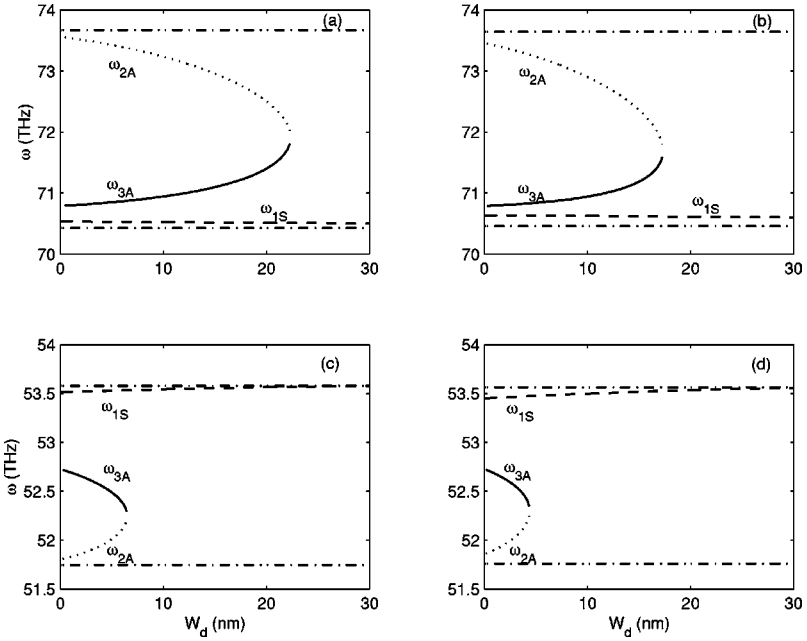

FIG. 3. Dependence of frequency of the localized IOPM's on the width W_d of the defect layer d: (a) and (b) correspond to the localized IOPM's lying in the AlAs-like minigap for $q_{//}W_a=0.6$ and 0.8; (c) and (d) correspond to the localized IOPM's lying in the GaAs-like minigap for $q_{//}W_a=0.6$ and 0.8, respectively. Here, we take $W_a=20$ nm, $W_b=8$ nm, and $x=0.25$. Explanations for all curves are the same as for Fig. 1.

understood that there are more than two localized IOPM's appearing inside each minigap. Moreover, we find that in the limit ($q_z=0$, and $q_{//}\rightarrow 0$) of the long wavelength the ω_{3A} branch approaches the LO frequency of $Al_xGa_{1-x}As$. This implies that the ω_{3A} originates from the ternary mixed crystals defect layers. In fact, there exist three localized IOPM's in AlAs-like minigap for certain concentration extent of x, but beyond this concentration extent, only two localized IOPM's or even one are survival. When $x=0$ or 1, the results are the same as those of binary structural defect SL presented in Ref. 24. When a(GaAs) and b(AlAs) are permuted, similar phenomena are observed. It is interesting to note from Fig. 1 that, with the increase of the concentration x, ω_{3A} branch shifts towards the higher-frequency region, meanwhile ω_{2A} branch shifts towards the low-frequency region. Furthermore, both modes ω_{2A} and ω_{3A} degenerate at certain values between $0.317<x<0.318$ for certain transverse wave number $q_{//}$. When $q_{//}$ is increased, ω_{2A} and ω_{3A} are separated into two branches again. When further increasing x, ω_{2A} and ω_{3A} are divided into two parts [see Fig. 1(c)]. Both the degeneracy positions of ω_{2A} and ω_{3A} at the left and right parts are varied with the concentration x and transverse wave number $q_{//}$. The larger the x, the wider the spacing between two degeneracy positions is. When the concentration x is increased to certain value, ω_{2A} and ω_{3A} at the right part are joined together and then it is difficult to distinguish them [see Fig. 1(d)]. The ω_{2A} and ω_{3A} are coupled together when they meet with each other, while ω_{1S} is not coupled

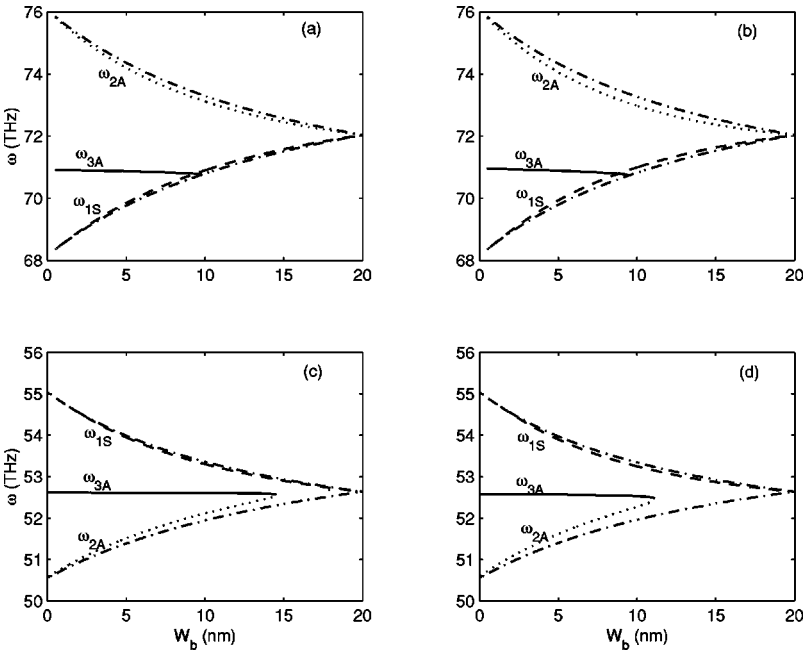

FIG. 4. Dependence of frequency of the localized IOPM's on the width W_b of the constituent layer b: (a) and (b) correspond to localized IOPM's lying in the AlAs-like minigap for $q_{//}W_a=0.6$ and 0.8; (c) and (d) correspond to localized IOPM's lying in the GaAs-like minigap for $q_{//}W_a=0.6$ and 0.8, respectively. Here, we take $W_a=20$ nm, $W_d=3$ nm, and $x=0.25$. Explanations for all curves are the same as for Fig. 1.

with ω_{2A} or ω_{3A}. This infers that both antisymmetric modes ω_{2A} and ω_{3A} possess the same orientation of the polarization and the orientation of the polarization of symmetric modes ω_{1S} is perpendicular to that of antisymmetric modes ω_{2A} and ω_{3A}. It gives again a strong support of the conclusion drawn in Ref. 24 that the localized IOPM's with symmetric or antisymmetric characteristics correspond to the longitudinal and transverse vibrations, respectively. For the special case $q_{//}=0$, we can conclude that symmetric mode ω_{1S} is of LO mode polarized parallel to the superlattice axis and antisymmetric modes ω_{2A} and ω_{3A} are of TO modes polarized in the plane of the layers. It should be noted that the ω_{1S} branch does not vary with x. This implies that the ω_{1S} branch originates from AlAs modes in the constituent layer.

For GaAS-like localized IOPM's depicted in Fig. 2, similar features are observed except that the frequency positions of ω_{1S}, ω_{2A}, and ω_{3A} branches are just reversed.

Figure 3 illustrates the frequencies of the localized IOPM's as a function of the W_d for different transverse $q_{//}$. With the increase of W_d, both ω_{2A} and ω_{3A} gradually approach each other and they degenerate at $W_d=22.25$ nm in Fig. 3(a), $W_d=17.25$ nm in Fig. 3(b), $W_d=6.45$ nm in Fig. 3(c), and $W_d=4.35$ nm in Fig. 3(d), respectively. Then ω_{2A} and ω_{3A} vanish and only ω_{1S} is left. It is not difficult to understand these behaviors after carefully observing the evolution of both ω_{2A} and ω_{3A} with the increase of the concentration x and the transverse wave number $q_{//}$ in Fig. 1, where the spacing between the left and right degeneracy points is produced and both ω_{2A} and ω_{3A} vanish. The width of W_d corresponding to the degeneracy point is different for different transverse wave numbers $q_{//}$ and concentrations x. With the increase of $q_{//}$, the degeneracy position of ω_{2A} and ω_{3A} lying in the AlAs-like minigap shifts towards narrower width W_d. Similar results are found for that lying in the GaAs-like minigap.

We now turn to investigate the influence of the width W_b on the localized IOPM's for different transverse $q_{//}$, shown in Fig. 4. It is well known from Ref. 24 that both ω_{1S} and ω_{2A} always appear in pairs inside each frequency minigap when the structural defect layer consists of AlAs or GaAs. The emergence of ω_{3A} is due to the introduction of ternary mixed-crystal defect layer. Meanwhile the ω_{2A} with the same asymmetry as ω_{3A} always shifts towards ω_{3A}. The degeneracy always occurs when ω_{2A} and ω_{3A} meet with each other. From Fig. 4, it is seen that the ω_{3A} is almost not influenced by the width W_b.

In summary, we have systematically investigated the properties of the localized IOPM's in AlAs-GaAs SL's with defect layer consisting of ternary mixed crystal $Al_xGa_{1-x}As$. We find that, in comparison with the previous work,[24] a new localized IOPM ω_{3A} with antisymmetry appears in each frequency minigap for certain parameters and it sensitively depends on the concentration x, the transverse wave number $q_{//}$, and the width of the defect layer, but it is not quite affected by the width of constituent layer. Another antisymmetric localized mode ω_{2A} also sensitively depends on the width of the constituent layers. Symmetric mode ω_{1S} seems not to be influenced by ternary mixed-crystal defect layer. Both antisymmetric modes ω_{2A} and ω_{3A} always degenerate as soon as they meet with each other in frequencies, while the symmetric mode ω_{1S} is not coupled with the antisymmetric modes ω_{2A} and ω_{3A}. Our studies show that the symmetric mode ω_{1S} is of LO mode polarized parallel to the superlattice axis and the antisymmetric modes ω_{2A} and ω_{3A} are of TO modes polarized in the plane of the layers for $q_{//}=0$.

This work was supported by the National Natural Science Foundation of China.

*Email address: kqchen@phys.tsinghua.edu.cn

[1] C. Colvard, T.A. Gaut, M.V. Klein, R. Merlin, R. Fischer, H. Morkoc, and A.C. Gossard, Phys. Rev. B **31**, 2080 (1985).
[2] R.E. Camley and D.L. Mills, Phys. Rev. B **29**, 1695 (1984).
[3] J.E. Zucker, A. Pinczuk, D.S. Chemla, A. Gossard, and W. Wiegmann, Phys. Rev. Lett. **53**, 1280 (1984).
[4] N. Mori and T. Ando, Phys. Rev. B **40**, 6175 (1989).
[5] Wenhui Duan, Jia-Lin Zhu, and Bing-Lin Gu, Phys. Rev. B **49**, 14 403 (1994).
[6] Bing-Lin Gu, Wenhui Duan, Shiying Xiong, and Youjiang Guo, Phys. Rev. B **54**, 16 983 (1996).
[7] Ruisheng Zheng and Mitsuru Matsuura, Phys. Rev. B **60**, 4937 (1999).
[8] K. Huang and B.F. Zhu, Phys. Rev. B **38**, 2183 (1988); **38**, 13 377 (1988).
[9] B.K. Ridley, Phys. Rev. B **39**, 5282 (1989).
[10] S. Rudin and T.L. Reinecke, Phys. Rev. B **41**, 7713 (1990).
[11] K.J. Nash, Phys. Rev. B **46**, 7723 (1992).
[12] Se Gi Yu, K.W. Kim, Michael A. Stroscio, G.J. Iafrate, J.-P. Sun, and G.I. Haddad, J. Appl. Phys. **82**, 3363 (1997).
[13] A.K. Sood, J. Menendez, M. Cardona, and K. Ploog, Phys. Rev. Lett. **54**, 2115 (1985).
[14] A. Ambrazevicius, M. Cardona, R. Merlin, and K. Ploog, Solid State Commun. **65**, 1035 (1988).
[15] A. Fainstein, P. Etchegoin, M.P. Chaamberlain, M. Cardona, K. Totemeyer, and K. Ebert, Phys. Rev. B **51**, 14 448 (1995).
[16] A.J. Shields, M.P. Chamberlain, M. Cardona, and K. Eberl, Phys. Rev. B **51**, 17 728 (1995).
[17] S. Mizuno and S.I. Tamura, Phys. Rev. B **45**, 13 423 (1992); **53**, 4549 (1996).
[18] G.P. Schwartz, G.J. Gualtieri, and W.A. Sunder, Appl. Phys. Lett. **58**, 971 (1991).
[19] R. James, S.M. Woodley, C.M. Dyer, and V.F. Humphrey, J. Acoust. Soc. Am. **97**, 2041 (1995).
[20] D. Bria, E.H. El Boudouti, A. Nougaoui, B. Djafari-Rouhani, and V.R. Velasco, Phys. Rev. B **60**, 2505 (1999); **61**, 15 858 (2000).
[21] Ke-Qiu Chen, Xue-Hua Wang, and Ben-Yuan Gu, Phys. Rev. B **61**, 12 075 (2000).
[22] R.E. Camley and D.L. Mills, Phys. Rev. B **29**, 1695 (1984).
[23] J. Mendialdua, A. Rodriguez, M. More, A. Akjoug, and L. Dobrzynski, Phys. Rev. B **50**, 14 605 (1994).
[24] Ke-Qiu Chen, Xue-Hua Wang, and Ben-Yuan Gu, Phys. Rev. B **62**, 9919 (2000).
[25] S. Adachi, J. Appl. Phys. **58**, R1 (1985).
[26] I.F. Chang and S.S. Mitra, Adv. Phys. **20**, 359 (1971).
[27] R. Chen, D.L. Lin, and Thomas F. George, Phys. Rev. B **41**, 1435 (1990).